Nonlinear random resistor diode networks and fractal dimensions of directed percolation clusters

Olaf Stenull and Hans-Karl Janssen
Institut für Theoretische Physik III, Heinrich-Heine-Universität, Universitätsstraße 1, 40225 Düsseldorf, Germany
(Received 1 February 2001; published 28 June 2001)

We study nonlinear random resistor diode networks at the transition from the nonpercolating to the directed percolating phase. The resistorlike bonds and the diodelike bonds under forward bias voltage obey a generalized Ohm's law $V \sim I^r$. Based on general grounds such as symmetries and relevance we develop a field theoretic model. We focus on the average two-port resistance, which is governed at the transition by the resistance exponent ϕ_r. By employing renormalization group methods we calculate ϕ_r for arbitrary r to one-loop order. Then we address the fractal dimensions characterizing directed percolation clusters. Via considering distinct values of the nonlinearity r, we determine the dimension of the red bonds, the chemical path, and the backbone to two-loop order.

DOI: 10.1103/PhysRevE.64.016135 PACS number(s): 64.60.Ak, 05.60.−k, 72.80.Ng

I. INTRODUCTION

Percolation [1] describes the passage of an influence through a medium that is irregularly structured in the sense that the influence can propagate through some regions whereas it cannot pass other areas. Prominent examples of such media are computer networks like the internet where information propagates and irregularity can be caused by random switch failures or other technical problems.

A particularly simple percolation model is the random resistor network (RRN). In this model the irregular medium is given by a, say, hypercubic lattice in which bonds between nearest neighboring sites are randomly occupied with a probability p. The influence corresponds to an external current I, which is injected at a terminal site x and withdrawn at another terminal site x'. Depending on the occupation probability p the resistors (bonds) are likely to either be isolated or form clusters. Two sites belong to the same cluster if they are connected by a path of bonds and hence current can flow between them. At low p two infinitely separated terminal sites x and x' are not connected by such a path and the network behaves as an insulator. For large p, on the other hand, many paths between x and x' may exist and the network is a conductor. Therefore, at some probability in between, a threshold p_c must exist where for the first time current can percolate from x to x'. The threshold probability is called the percolation threshold. Since it separates the conducting and the insulating phase, it is also referred to as the critical probability. In RRNs the influence can percolate through occupied bonds in all directions. The resulting clusters are typically isotropic in space. This kind of percolation is referred to as isotropic percolation (IP). The linear extent of the isotropic clusters can be characterized by the correlation length $\xi \sim |p-p_c|^{-\nu}$, where ν is the correlation length exponent of the IP universality class.

Directed percolation (DP) [2] is an anisotropic variant of percolation. The bonds function as diodes so that the current can percolate only along a given distinguished direction. The critical properties of isotropic and directed percolation are very different. Typical DP clusters are anisotropic and they are characterized by two different correlation lengths: $\xi_\parallel$ (parallel to the distinguished direction) and $\xi_\perp$ (perpendicular to it). As one approaches the critical probability, the two correlation lengths diverge with the exponents $\nu_\parallel$ and $\nu_\perp$ of the DP universality class.

The apparent success of DP might be attributed to the fact that it is perhaps the simplest model resulting in branching self-affine objects. It has many potential applications, including fluid flow through porous media under gravity, hopping conductivity in a strong electric field [3], crack propagation [4], and the propagation of surfaces at depinning transitions [5].

DP has a dynamic interpretation in which the distinguished direction is viewed as time. A DP cluster then represents the history of a stochastic process. In this dynamic interpretation the DP universality class is the generic universality class for phase transitions from an active to an absorbing inactive state. For example, the epidemic spreading of an infectious desease without immunization [6] may be described by DP [7]. Moreover, DP is related to self-organized critical models [8].

In the early 1980s Redner [9–11] introduced the random resistor diode network (RDN) which comprises both IP and DP. A RDN is a bond percolation model where nearest neighbor sites are connected by a resistor, a positive diode (conducting only in the distinguished direction), a negative diode (conducting only opposite to the distinguished direction), or an insulator with respective probabilities p, p_+, p_-, and $q=1-p-p_+-p_-$. In the three-dimensional phase diagram (pictured as a tetrahedron spanned by the four probabilities) one finds a nonpercolating and three percolating phases. The percolating phases are isotropic, positively directed, or negatively directed. Between the phases there are surfaces of continuous transitions. All four phases meet along a multicritical line, where $0 \leqslant r := p_+ = p_- \leqslant 1/2$ and $p = p_c(r)$. On the entire multicritical line, i.e., independently of r, one finds the scaling properties of the usual isotropic percolation ($r=0$). For the crossover from IP to DP see, e.g., Ref. [12]. In this paper we focus exclusively on the vicinity of the critical surface separating the nonpercolating and the positively directed phase.

An important notion in the theory of RDNs is the average

resistance $M_R(x,x')$ between two connected terminal sites $x=(x_\perp,t)$ and $x'=(x'_\perp,t')$ of the network. The critical behavior of this average resistance is well known [13,14]. If $M_R(x,x')$ is measured, for example, in the distinguished, timelike direction then it scales as

$$M_R(x,x')\sim|t-t'|^{\phi/\nu_\parallel}, \tag{1.1}$$

with ϕ being the DP resistance exponent. Here in this paper we consider a generalized RDN in which the resistorlike bonds and the diodelike bonds under forward bias voltage obey a generalized Ohm's law $V\sim I^r$. Our motivation for assuming this nonlinear Ohm's law is twofold. First, real circuit elements have nonlinear current-voltage characteristics. This is obviously the case for diodes but it also applies to a certain extent to resistors, in particular for large currents. Our main motivation is, however, that the generalized average resistance $M_{R_r}(x,x')$ is related for certain values of r to important fractal substructures of DP clusters. This relation provides us with an elegant way to determine the fractal dimensions of the red bonds, the chemical path, and the DP backbone. Parts of this work were presented briefly in Ref. [13].

The plan of presentation is the following. In Sec. II we give background on nonlinear RDNs and set up our field theoretic model. Section III sketches our renormalization group improved perturbation calculation. We derive the scaling behavior of $M_{R_r}(x,x')$, which is governed by a generalized resistance exponent ϕ_r. We present our one-loop result for ϕ_r. In Sec. IV we calculate the fractal dimensions of the red bonds, the chemical path, and the DP backbone by considering the limits $r\to\infty$, $r\to 0^+$, and $r\to -1^+$, respectively. Section V contains our conclusions.

II. THE MODEL

A. Generalized Ohm's law

Consider a d-dimensional hypercubic lattice in which the direction $\mathbf{n}=1/\sqrt{d}(1,\ldots,1)$ is distinguished. Assume that the bonds $\underline{b}_{\langle i,j\rangle}$ between two nearest neighboring sites i and j are directed so that $b_{\langle i,j\rangle}\cdot\mathbf{n}>0$.

Suppose that the directed bonds obey the nonlinear Ohm's law [15]

$$\sigma_{\underline{b}_{\langle i,j\rangle}}(V_{\underline{b}_{\langle i,j\rangle}})V_{\underline{b}_{\langle i,j\rangle}}|V_{\underline{b}_{\langle i,j\rangle}}|^{s-1}=I_{\underline{b}_{\langle i,j\rangle}}, \tag{2.1a}$$

or, equivalently,

$$V_{\underline{b}_{\langle i,j\rangle}}=\rho_{\underline{b}_{\langle i,j\rangle}}(I_{\underline{b}_{\langle i,j\rangle}})I_{\underline{b}_{\langle i,j\rangle}}|I_{\underline{b}_{\langle i,j\rangle}}|^{r-1}. \tag{2.1b}$$

$V_{\underline{b}_{\langle i,j\rangle}}=V_j-V_i$, where V_i denotes the potential at site i, is the voltage drop over the bond between sites i and j. $I_{\underline{b}_{\langle i,j\rangle}}$ denotes the current flowing from j to i. In the following we drop the subscript $\langle i,j\rangle$ whenever the meaning is clear. The bond conductances $\sigma_{\underline{b}}$ are random variables taking on the values σ, $\sigma\theta(V)$, $\sigma\theta(-V)$, and 0 with respective probabilities p, p_+, p_-, and q. σ is a positive constant and θ denotes the Heaviside function. The exponents r and s describe the nonlinearity with $r=s^{-1}$. The bond resistances $\rho_{\underline{b}}$ are related to the conductances via $\sigma_{\underline{b}}=\rho_{\underline{b}}^{-s}$. Note that the diodes are idealized: under forward bias voltage they behave for $r=1$ as ''Ohmic'' resistors whereas they are insulating under backward bias voltage. We point out that the parentheses in Eq. (2.1) contain the argument of the bond conductance or resistance, respectively. It is important to realize that these quantities depend on the voltages or currents by means of the step function and that $\mathrm{sgn}(V_{\underline{b}})=\mathrm{sgn}(I_{\underline{b}})$. Hence we may write $\sigma_{\underline{b}}(V_{\underline{b}})=\sigma_{\underline{b}}(I_{\underline{b}})$ and $\rho_{\underline{b}}(I_{\underline{b}})=\rho_{\underline{b}}(V_{\underline{b}})$.

Assume that an external current I is injected at x and withdrawn at x'. It is understood that x and x' are connected. The power dissipated on the network is by definition

$$P=I(V_x-V_{x'}). \tag{2.2}$$

Using Ohm's law it may be expressed entirely in terms of the voltages as

$$\begin{aligned}P&=R_{r,+}(x,x')^{-1}|V_x-V_{x'}|^{s+1}\\&=\sum_{\underline{b}}\sigma_{\underline{b}}(V_{\underline{b}})|V_{\underline{b}}|^{s+1}\\&=P(\{V\}).\end{aligned} \tag{2.3}$$

The sum is taken over all bonds on the cluster connecting x and x' and $\{V\}$ denotes the corresponding set of voltages. $R_{r,+}(x,x')$ stands for the macroscopic resistance when I is inserted at x and withdrawn at x'. Similarly one may define $R_{r,-}(x,x')$ as the macroscopic resistance when I is inserted at x' and withdrawn at x. The two quantities are related by $R_{r,+}(x,x')=R_{r,-}(x',x)$. From the power one obtains Kirchhoff's first law

$$\sum_{\langle j\rangle}\sigma_{\underline{b}_{\langle i,j\rangle}}(V_{\underline{b}_{\langle i,j\rangle}})V_{\underline{b}_{\langle i,j\rangle}}|V_{\underline{b}_{\langle i,j\rangle}}|^{s-1}=\sum_{\langle j\rangle}I_{\underline{b}_{\langle i,j\rangle}}=-I_i \tag{2.4}$$

as a consequence of the variation principle

$$\frac{\partial}{\partial V_i}\left[\frac{1}{s+1}P(\{V\})+\sum_k I_kV_k\right]=0. \tag{2.5}$$

The summation in Eq. (2.4) extends over the nearest neighbors of i and I_i is given by $I_i=I(\delta_{i,x}-\delta_{i,x'})$.

Alternatively to Eq. (2.3), the power can be expressed in terms of the currents as

$$P=R_{r,+}(x,x')|I|^{r+1}=\sum_{\underline{b}}\rho_{\underline{b}}(I_{\underline{b}})|I_{\underline{b}}|^{r+1}=P(\{I\}), \tag{2.6}$$

with $\{I\}$ denoting the set of currents flowing through the individual bonds. It is understood that $\rho_{\underline{b}}(I_{\underline{b}})|I_{\underline{b}}|^{r+1}=0$ whenever $\sigma_{\underline{b}}(I_{\underline{b}})=0$. Kirchhoff's second law, saying that the voltage drops along closed loops vanish, can be stated in terms of the variation principle

$$\frac{\partial}{\partial I^{(l)}}P(\{I^{(l)}\},I)=0, \tag{2.7}$$

i.e., there are no independent loop currents $I^{(l)}$ circulating around a complete set of independent closed loops.

B. Relation to fractal substructures

Now we take a short detour and show that the average resistance $M_{R_r}(x,x')$ is related for specific values of r to the mass, i.e., the average number of bonds, of important substructures of DP clusters. The arguments below are well established for RRNs and we simply adapt them here to RDNs. We start with the backbone. The (forward) backbone between two sites x and x' is defined, in principle, as the union of all current carrying bonds when I is injected at x and withdrawn at x'. Consider $r\to -1^+$. One obtains immediately as a consequence of Eq. (2.6) that

$$R_{-1,+}(x,x')=\lim_{r\to -1^+}\sum_{\underline{b}}\rho_{\underline{b}}(I_{\underline{b}})\left|\frac{I_{\underline{b}}}{I}\right|^{r+1}=\sum_{\underline{b}}\rho_{\underline{b}}(I_{\underline{b}}), \tag{2.8}$$

with only those bonds carrying nonzero current contributing to the sum on the right hand side. Hence

$$\lim_{r\to -1^+} M_{R_r}(x,x')\sim M_B, \tag{2.9}$$

where M_B stands for the mass of the backbone.

Now we turn to $r\to\infty$ and $r\to 0^+$ following the lines of Blumenfeld and Aharony [16]. On the backbone between two sites x and x' one may distinguish between two different substructures: blobs formed by multiconnected bonds and singly connected bonds, which are referred to as red bonds. Both substructures contribute to the resistance of the backbone,

$$R_{r,+}(x,x')=\sum_{\underline{b}}^{\text{blob}}\rho_{\underline{b}}(I_{\underline{b}})\left|\frac{I_{\underline{b}}}{I}\right|^{r+1}+\sum_{\underline{b}}^{\text{red}}\rho_{\underline{b}}(I_{\underline{b}}), \tag{2.10}$$

where the sums are taken over all bonds belonging to blobs and over all red bonds, respectively. Since sites on a blob are multiconnected by definition, $|I_{\underline{b}}|<|I|$, and thus

$$\lim_{r\to\infty}\sum_{\underline{b}}^{\text{blob}}\rho_{\underline{b}}(I_{\underline{b}})\left|\frac{I_{\underline{b}}}{I}\right|^{r+1}=0. \tag{2.11}$$

In conclusion, $M_{R_r}(x,x')$ is related to the mass of the red bonds M_{red} via

$$\lim_{r\to\infty} M_{R_r}(x,x')\sim M_{\text{red}}. \tag{2.12}$$

Consider now the first site x at some end of a blob. An entering current I splits into currents $I_{i,x}$ flowing to nearest neighbors i with

$$|I_{i,x}|=\sigma_{i,x}(V_x-V_i)|V_x-V_i|^s. \tag{2.13}$$

In the limit $s\to\infty$ the ratios $|I_{i,x}|/|I_{j,x}|$ vanish whenever $\sigma_{i,x}(V_x-V_i)|V_x-V_i|^s<\sigma_{j,x}(V_x-V_j)|V_x-V_j|^s$. Thus, current flows only through the resistor with the largest $\sigma_{i,x}(V_x-V_i)|V_x-V_i|^s$. This argument may be iterated throughout the entire blob. One identifies either a single self-avoiding chain through which I flows, with

$$P_r=\sum_{\underline{b}}\rho_{\underline{b}}(I_{\underline{b}})|I|^{r+1} \tag{2.14}$$

being the power dissipated on the chain, or several such chains with identical power. The expression in Eq. (2.14) is minimal for minimal $\Sigma_{\underline{b}}\rho_{\underline{b}}$, i.e., the current chooses the shortest path through the blob, and one is led to

$$\lim_{r\to 0^+} M_{R_r}(x,x')\sim M_{\min}, \tag{2.15}$$

where $M_{\min}$ stands for the mass of the chemical path.

C. Replica technique

Our aim now is to calculate the average resistance between two ports x and x', which is precisely defined by

$$M_{R_r}(x,x')=\langle\chi_+(x,x')R_{r,+}(x,x')\rangle_C/\langle\chi_+(x,x')\rangle_C. \tag{2.16}$$

$\langle\cdots\rangle_C$ denotes the average over all configurations of the diluted lattice. $\chi_+(x,x')$ is an indicator function that takes the value 1 if x and x' are positively connected, i.e., if I can percolate from x to x', and zero otherwise. Note that $\langle\chi_+(x,x')\rangle_C=\langle\chi_-(x',x)\rangle_C$ is nothing more than the usual DP correlation function.

Now we follow an idea by Stephen [17] and its generalization to networks of nonlinear resistors by Harris [18] and exploit the correlation functions

$$G(x,x',\vec{\lambda})=\langle\psi_{\vec{\lambda}}(x)\psi_{-\vec{\lambda}}(x')\rangle_{\text{rep}} \tag{2.17}$$

of

$$\psi_{\vec{\lambda}}(x)=\exp(i\vec{\lambda}\cdot\vec{V}_x),\quad \vec{\lambda}\neq\vec{0}, \tag{2.18}$$

as generating functions of M_{R_r}. In writing Eqs. (2.17) and (2.18) we switched to D-fold replicated voltages $V_i\to\vec{V}_i=(V_i^{(1)},\ldots,V_i^{(D)})$, and currents $\lambda_i=iI_i\to\vec{\lambda}_i=(\lambda_i^{(1)},\ldots,\lambda_i^{(D)})$. The correlation functions are given by

$$G(x,x',\vec{\lambda})=\left\langle Z^{-D}\int\prod_j\prod_{\alpha=1}^{D}dV_j^{(\alpha)}\exp\left[-\frac{1}{s+1}P(\{\vec{V}\})+\frac{i\omega}{2}\sum_i\vec{V}_i^2+i\vec{\lambda}\cdot(\vec{V}_x-\vec{V}_{x'})\right]\right\rangle_C, \tag{2.19}$$

where

$$P(\{\vec{V}\})=\sum_{\alpha=1}^{D}P(\{V^{(\alpha)}\})=\sum_{\alpha=1}^{D}\sum_{\underline{b}}\sigma_{\underline{b}}(V_{\underline{b}}^{(\alpha)})|V_{\underline{b}}^{(\alpha)}|^{s+1} \tag{2.20}$$

and Z is the normalization

$$Z=\int \prod_j dV_j \exp\left[-\frac{1}{s+1}P(\{V\})+\frac{i\omega}{2}\sum_i V_i^2\right]. \tag{2.21}$$

The additional power term $(i\omega/2)\Sigma_i V_i^2$ that we have introduced in Eqs. (2.19) and (2.21) is necessary to give the voltage integrals a well defined meaning. Without this term the integrands depend only on voltage differences and the integrals are divergent. Physically, the new term corresponds to grounding each lattice site by a capacitor of unit capacity. The original situation can be retrieved by taking the limit of vanishing frequency, $\omega\to 0$.

Because the integrations in Eqs. (2.19) and (2.21) are not Gaussian, we employ the saddle point method. The saddle point equation is nothing more than the variation principle stated in Eq. (2.5). Thus, the maximum of the integrand is determined by the solution of the circuit equations (2.4). Provided that the condition $|I|^{r+1}\gg\sigma$ holds, we obtain, up to an unimportant multiplicative constant which goes to 1 in the limit $D\to 0$,

$$G(x,x',\vec{\lambda})=\left\langle \exp\left[\frac{\Lambda_r(\vec{\lambda})}{r+1}R_{r,+}(x,x')\right]\right\rangle_C, \tag{2.22}$$

where

$$\Lambda_r(\vec{\lambda})=\sum_{\alpha=1}^{D}(-i\lambda^{(\alpha)})^{r+1}. \tag{2.23}$$

Now we may expand G about $\Lambda_r(\vec{\lambda})=0$,

$$G(x,x',\vec{\lambda})=\langle\chi_+(x,x')\rangle_C\left(1+\frac{\Lambda_r(\vec{\lambda})}{r+1}M_{R_r}(x,x')+\cdots\right). \tag{2.24}$$

This shows us that G is indeed the desired generating function from which the average resistance may be calculated via

$$M_{R_r}(x,x')=\langle\chi_+(x,x')\rangle_C^{-1}\frac{\partial}{\partial(\Lambda_r(\vec{\lambda})/(r+1))}\times G(x,x',\vec{\lambda})|_{\Lambda_r(\vec{\lambda})=0}. \tag{2.25}$$

Here we would like to comment on the nature of $\vec{\lambda}$. We work near the limit when all the components of $\vec{\lambda}$ are equal and continue to large imaginary values. Accordingly we set [18]

$$\lambda^{(\alpha)}=i\lambda_0+\xi^{(\alpha)} \tag{2.26}$$

with real λ_0 and $\xi^{(\alpha)}$, and impose the condition $\Sigma_{\alpha=1}^{D}\xi^{(\alpha)}=0$. The saddle point approximation may be justified by demanding

$$|\lambda_0|\gg 1. \tag{2.27}$$

Substitution of Eq. (2.26) into the definition of Λ_r leads to

$$\Lambda_r(\vec{\lambda})=\sum_{\alpha=1}^{D}\left\{\lambda_0^{r+1}-i(r+1)\lambda_0^r\xi^{(\alpha)}-\frac{r(r+1)}{2}\lambda_0^{r-1}\xi^{(\alpha)2}+\cdots\right\}=D\lambda_0^{r+1}-\frac{r(r+1)}{2}\lambda_0^{r-1}\vec{\xi}^{\,2}+\cdots. \tag{2.28}$$

Thus, one can justify the expansion in Eq. (2.24) by invoking the conditions

$$|\lambda_0|^{r+1}\ll D^{-1} \quad\text{and}\quad |\lambda_0|^{r-1}\vec{\xi}^{\,2}\ll 1. \tag{2.29}$$

Note that the replica limit $D\to 0$ allows for a simultaneous fulfillment of the conditions (2.27) and (2.29). However, we will not rely exclusively on these conditions on $\vec{\lambda}$. We will provide several consistency checks for the validity of Harris's saddle point approach as we go along and reproduce known results.

D. Field theoretic Hamiltonian

Since infinite voltage drops between different clusters may occur, it is not guaranteed that Z stays finite, i.e., the limit $\lim_{D\to 0}Z^D$ is not well defined. This problem can be regularized by switching to voltage variables $\vec{\vartheta}$ taking discrete values on a D-dimensional torus [19]. The voltages are discretized by setting $\vec{\vartheta}=\Delta\vartheta\vec{k}$, where $\Delta\vartheta=\vartheta_M/M$ is the gap between successive voltages, ϑ_M is a voltage cutoff, $\vec{k}$ is a D-dimensional integer, and M a positive integer. The components of $\vec{k}$ are restricted to $-M<k^{(\alpha)}\leqslant M$ and periodic boundary conditions are realized by setting $k^{(\alpha)}=k^{(\alpha)}\mathrm{mod}(2M)$. The continuum may be restored by taking $\vartheta_M\to\infty$ and $\Delta\vartheta\to 0$. By setting $\vartheta_M=\vartheta_0 M$, $M=m^2$, and, respectively, $\Delta\vartheta=\vartheta_0/m$, the two limits can be taken simultaneously via $m\to\infty$. Note that the limit $D\to 0$ has to be taken before any other limit. Since the voltages and $\vec{\lambda}$ are conjugated variables, $\vec{\lambda}$ is affected by the discretization as well:

$$\vec{\lambda}=\Delta\lambda\vec{l}, \quad \Delta\lambda\Delta\vartheta=\pi/M, \tag{2.30}$$

where $\vec{l}$ is a D-dimensional integer taking the same values as $\vec{k}$. This choice guarantees that the completeness and orthogonality relations

$$\frac{1}{(2M)^D}\sum_{\vec{\vartheta}}\exp(i\vec{\lambda}\cdot\vec{\vartheta})=\delta_{\vec{\lambda},\vec{0}\ \mathrm{mod}(2M\Delta\lambda)} \tag{2.31a}$$

and

$$\frac{1}{(2M)^D}\sum_{\vec{\lambda}}\exp(i\vec{\lambda}\cdot\vec{\vartheta})=\delta_{\vec{\vartheta},\vec{0}\ \mathrm{mod}(2M\Delta\vartheta)} \tag{2.31b}$$

do hold. Equation (2.31) provides us with a Fourier transform between the $\vec{\vartheta}$- and $\vec{\lambda}$-tori.

After taking care of these regularization issues, we now carry out the average over the diluted lattice configurations in Eq. (2.19). This provides us with the effective Hamiltonian

$$H_{\rm rep}=-\ln\left\langle \exp\left[-\frac{1}{s+1}P(\{\vec{\vartheta}\})+\frac{i\omega}{2}\sum_i \vec{\vartheta}_i^2\right]\right\rangle_C$$
$$=-\sum_{\underline{b}} K(\vec{\vartheta}_{\underline{b}})-\frac{i\omega}{2}\sum_i \vec{\vartheta}_i^2, \tag{2.32}$$

where

$$K(\vec{\vartheta})=\ln\Bigg\{q+p\prod_{\alpha=1}^{D}\exp\left[-\frac{\sigma}{s+1}|\vartheta^{(\alpha)}|^{s+1}\right]$$
$$+p_+\prod_{\alpha=1}^{D}\exp\left[-\frac{\sigma}{s+1}\theta(\vartheta^{(\alpha)})|\vartheta^{(\alpha)}|^{s+1}\right]$$
$$+p_-\prod_{\alpha=1}^{D}\exp\left[-\frac{\sigma}{s+1}\theta(-\vartheta^{(\alpha)})|\vartheta^{(\alpha)}|^{s+1}\right]\Bigg\}. \tag{2.33}$$

In order to proceed further we recall the choice for $\vec{\lambda}$ made in Eq. (2.26). Because $\vec{\lambda}$ and $\vec{\vartheta}$ are related by Ohm's law, we have to make a consistant choice for $\vec{\vartheta}$:

$$\vartheta^{(\alpha)}=\vartheta_0+\zeta^{(\alpha)}, \tag{2.34}$$

with real ϑ_0 and $\zeta^{(\alpha)}$, and where $\Sigma_{\alpha=1}^{D}\zeta^{(\alpha)}=0$. Upon imposing the condition

$$|\vartheta_0|\gg|\zeta^{(\alpha)}| \tag{2.35}$$

for all α we may write

$$K(\vec{\vartheta})=\ln\Bigg\{q+p\exp\left(-\frac{\sigma}{s+1}|\vartheta|^{s+1}\right)$$
$$+p_+\left[\theta(-\vartheta_0)+\theta(\vartheta_0)\exp\left(-\frac{\sigma}{s+1}|\vartheta|^{s+1}\right)\right]$$
$$+p_-\left[\theta(\vartheta_0)+\theta(-\vartheta_0)\exp\left(-\frac{\sigma}{s+1}|\vartheta|^{s+1}\right)\right]\Bigg\}, \tag{2.36}$$

where we have introduced the abbreviation $|\vartheta|^{s+1}=\Sigma_{\alpha=1}^{D}|\vartheta^{(\alpha)}|^{s+1}$. After doing a little straightforward algebra and by dropping a term

$$\theta(\vartheta_0)\ln[1-p-p_+]+\theta(-\vartheta_0)\ln[1-p-p_-] \tag{2.37}$$

that does not depend on the bond conductances, we obtain

$$K(\vec{\vartheta})=\theta(\vartheta_0)K_+(\vec{\vartheta})+\theta(-\vartheta_0)K_-(\vec{\vartheta}). \tag{2.38}$$

The $K_\pm(\vec{\vartheta})$ in Eq. (2.38) are given by

$$K_\pm(\vec{\vartheta})=\ln\left[1-\frac{p+p_\pm}{1-p-p_\pm}\exp\left(-\frac{\sigma}{s+1}|\vartheta|^{s+1}\right)\right]. \tag{2.39}$$

Note that these are exponentially decreasing functions in replica space with a decay rate proportional to σ^{-1}. In order to refine $H_{\rm rep}$ toward a field theoretic Hamiltonian we now expand $K(\vec{\vartheta})$ in terms of ψ:

$$K(\vec{\vartheta}_{\underline{b}})=\frac{1}{(2M)^D}\sum_{\vec{\lambda}}\sum_{\vec{\vartheta}}\exp[i\vec{\lambda}\cdot(\vec{\vartheta}_{\underline{b}}-\vec{\vartheta})]K(\vec{\vartheta}). \tag{2.40}$$

Upon exploiting that $\theta(\vartheta_0)=\theta(\lambda_0)$ we obtain

$$K(\vec{\vartheta}_{\underline{b}})=\sum_{\vec{\lambda}\neq\vec{0}}\psi_{\vec{\lambda}}(i)\psi_{-\vec{\lambda}}(j)\Bigg\{\frac{1}{2}[\tilde{K}_+(\vec{\lambda})+\tilde{K}_-(\vec{\lambda})]+\frac{1}{2}[\theta(\lambda_0)$$
$$-\theta(-\lambda_0)][\tilde{K}_+(\vec{\lambda})-\tilde{K}_-(\vec{\lambda})]\Bigg\}, \tag{2.41}$$

where $\tilde{K}_\pm(\vec{\lambda})$ stands for the Fourier transform of $K_\pm(\vec{\vartheta})$,

$$\tilde{K}_\pm(\vec{\lambda})=\frac{1}{(2M)^D}\sum_{\vec{\vartheta}}\exp[i\vec{\lambda}\cdot\vec{\vartheta}]K(\vec{\vartheta}). \tag{2.42}$$

The Fourier transform can be carried out by switching back to continuous currents and expanding the logarithm in Eq. (2.39). The result so obtained has the Taylor expansion

$$\tilde{K}_\pm(\vec{\lambda})=\tau_\pm-w_{r,\pm}\Lambda_r(\vec{\lambda})+\cdots, \tag{2.43}$$

where $\tau_\pm$ and $w_{r,\pm}\sim\sigma^{-1}$ are expansion coefficients depending on p and $p_\pm$ with $\tau_\pm(p,p_+,p_-)=\tau_\mp(p,p_-,p_+)$ and $w_{r,\pm}(p,p_+,p_-)=w_{r,\mp}(p,p_-,p_+)$. Now we insert Eq. (2.41) into Eq. (2.32). We also carry out a gradient expansion in position space. This is justified because only nearest neighbor pairs enter in the power P, i.e., the interaction is short ranged not only in replica but also in position space. We find

$$H_{\rm rep}=-\sum_{\vec{\lambda}\neq\vec{0}}\sum_{i,\underline{b}_i}\Bigg\{\frac{1}{2}[\tilde{K}_+(\vec{\lambda})+\tilde{K}_-(\vec{\lambda})]\psi_{-\vec{\lambda}}(i)$$
$$\times\left[1+\frac{1}{2}(\underline{b}_i\cdot\nabla)^2+\cdots\right]\psi_{\vec{\lambda}}(i)+\frac{1}{2}[\theta(\lambda_0)-\theta(-\lambda_0)]$$
$$\times[\tilde{K}_+(\vec{\lambda})-\tilde{K}_-(\vec{\lambda})]\psi_{-\vec{\lambda}}(i)[\underline{b}_i\cdot\nabla+\cdots]\psi_{\vec{\lambda}}(i), \tag{2.44}$$

with $\tilde{K}_\pm(\vec{\lambda})$ given by Eq. (2.43).

We proceed with the usual coarse graining step and replace the $\psi_{\vec{\lambda}}(i)$ by order parameter fields $\psi_{\vec{\lambda}}(\mathbf{x})$ which inherit the constraint $\vec{\lambda}\neq\vec{0}$. We model the corresponding field theoretic Hamiltonian $\mathcal{H}$ in the spirit of Landau as a mesoscopic free energy and introduce the Landau-Ginzburg-Wilson type functional

$$\mathcal{H}=\int d^dx\Bigg\{\frac{1}{2}\sum_{\vec{\lambda}\neq\vec{0}}\psi_{-\vec{\lambda}}(\mathbf{x})\{\tau-\nabla^2-w_r\Lambda_r(\vec{\lambda})+[\theta(\lambda_0)-\theta(-\lambda_0)]\mathbf{v}\cdot\nabla\}\psi_{\vec{\lambda}}(\mathbf{x})+\frac{g}{6}\sum_{\vec{\lambda},\vec{\lambda}',\vec{\lambda}+\vec{\lambda}'\neq\vec{0}}\psi_{-\vec{\lambda}}(\mathbf{x})\psi_{-\vec{\lambda}'}(\mathbf{x})\psi_{\vec{\lambda}+\vec{\lambda}'}(\mathbf{x})+\frac{i\omega}{2}\nabla^2_{\vec{\lambda}}\psi_{\vec{\lambda}}(\mathbf{x})\Bigg\}. \tag{2.45}$$

As usual we have neglected all terms that are irrelevant in the sense of the renormalization group. The parameter τ is the coarse grained ancestor of $\tau_+ + \tau_-$. It specifies the ''distance'' from the critical surface under consideration. $w_r \sim \sigma^{-1}$ is the coarse grained analog of $w_{r,+} + w_{r,-}$. The vector $\mathbf{v}$ lies in the distinguished direction, $\mathbf{v}=v\mathbf{n}$. v depends like τ and w_r on the three probabilities p, p_+, and p_-. For $p_+ = p_-$ it vanishes. In the limit $w_r \to 0$ our Hamiltonian $\mathcal{H}$ describes the usual purely geometric DP. Indeed, $\mathcal{H}$ leads for $w_r \to 0$ to exactly the same perturbation series as obtained in [20–22]. In the limit $r \to 1$ $\mathcal{H}$ describes resistor diode percolation as studied in Refs. [13,14]. In the remainder of this paper we drop the regularization term proportional to ω for simplicity.

III. RENORMALIZATION GROUP ANALYSIS

Now we are in the position to set up a perturbation calculation. This perturbation calculation can be simplified from the onset by manipulating $\mathcal{H}$ in such a way that it takes the form of a dynamic functional [23–25]. We assume that $v \neq 0$ and introduce new variables by setting

$$x_\parallel = \mathbf{n}\cdot\mathbf{x} = v\rho t, \quad \psi = |v|^{-1/2}s, \quad g = |v|^{1/2}\bar{g}. \tag{3.1}$$

By substituting Eq. (3.1) into Eq. (2.45) we obtain

$$\mathcal{J}=\int d^{d_\perp}x_\perp\, dt\Bigg\{\frac{1}{2}\sum_{\vec{\lambda}\neq\vec{0}}s_{-\vec{\lambda}}(\mathbf{x}_\perp,t)\Big[\rho[\tau-\nabla_\perp^2-w_r\Lambda_r(\vec{\lambda})]+[\theta(\lambda_0)-\theta(-\lambda_0)]\frac{\partial}{\partial t}\Big]s_{\vec{\lambda}}(\mathbf{x}_\perp,t)+\frac{\rho\bar{g}}{6}\sum_{\vec{\lambda},\vec{\lambda}',\vec{\lambda}+\vec{\lambda}'\neq\vec{0}}s_{-\vec{\lambda}}(\mathbf{x}_\perp,t)s_{-\vec{\lambda}'}(\mathbf{x}_\perp,t)s_{\vec{\lambda}+\vec{\lambda}'}(\mathbf{x}_\perp,t)\Bigg\}, \tag{3.2}$$

where $d_\perp = d-1$. Note that we have neglected a term containing a second derivative with respect to the ''time'' t. This is justified because this term is less relevant than the one with the first ''time'' derivative, which we kept.

We proceed with standard methods of field theory [26]. From Eq. (3.2) we gather the diagrammatic elements contributing to our perturbation series. The first element is the vertex $-\bar{g}$. Dimensional analysis shows that the vertex $\bar{g}$ is marginal in four transverse dimensions. Hence $d = d_\perp + 1 = 5$ is the upper critical dimension as is well known for DP. The second diagrammatic element is the Gaussian propagator $G(\mathbf{x}_\perp,t,\vec{\lambda})$ which is determined by the equation of motion

$$\Big\{\rho[\tau-\nabla^2-w_r\Lambda_r(\vec{\lambda})]+[\theta(\lambda_0)-\theta(-\lambda_0)]\frac{\partial}{\partial t}\Big\}G(\mathbf{x}_\perp,t,\vec{\lambda}) = \delta(\mathbf{x}_\perp)\delta(t). \tag{3.3}$$

For the Fourier transformed $\tilde{G}(\mathbf{p},t,\vec{\lambda})$ of $G(\mathbf{x}_\perp,t,\vec{\lambda})$, where $\mathbf{p}$ is the momentum conjugate to $\mathbf{x}_\perp$, one readily obtains

$$\tilde{G}(\mathbf{p},t,\vec{\lambda}) = \tilde{G}_+(\mathbf{p},t,\vec{\lambda}) + \tilde{G}_-(\mathbf{p},t,\vec{\lambda}). \tag{3.4}$$

The quantities on the right hand side are given by

$$\tilde{G}_\pm(\mathbf{p},t,\vec{\lambda}) = \theta(\pm t)\,\theta(\pm\lambda_0)\exp[\mp t\rho(\tau+\mathbf{p}^2-w_r\Lambda_r(\vec{\lambda}))]\times(1-\delta_{\vec{\lambda},\vec{0}}). \tag{3.5}$$

For the diagrammatic expansion it is sufficient to keep either $\tilde{G}_+(\mathbf{p},t,\vec{\lambda})$ or $\tilde{G}_-(\mathbf{p},t,\vec{\lambda})$. We choose to keep $\tilde{G}_+(\mathbf{p},t,\vec{\lambda})$.

A. Nonlinear resistance of Feynman diagrams

From the vertex $-\bar{g}$ and the propagator $\tilde{G}_+(\mathbf{p},t,\vec{\lambda})$ we now assemble the Feynman graphs constituting our diagrammatic expansion. As in our previous work on transport in IP [27–31] these Feynman diagrams have a real-world interpretation: they may be viewed as being directed resistor networks themselves. This real-world interpretation has basically two roots. The first one is that the principal propagator $\tilde{G}_+(\mathbf{p},t,\vec{\lambda})$ decomposes into two parts:

$$\tilde{G}_+(\mathbf{p},t,\vec{\lambda}) = \theta(t)\,\theta(\lambda_0)\exp[-t\rho(\tau+\mathbf{p}^2-w_r\Lambda_r(\vec{\lambda}))] - \theta(t)\exp[-t\rho(\tau+\mathbf{p}^2)]\,\delta_{\vec{\lambda},\vec{0}}. \tag{3.6}$$

One of these parts is carrying $\vec{\lambda}$'s and hence we call it conducting. The other one is not carrying $\vec{\lambda}$'s and accordingly we call it insulating. Equation (3.6) allows for a schematic decomposition of the principal diagrams into sums of conducting diagrams consisting of conducting and insulating propagators. In Fig. 1 we list the conducting diagrams resulting from the decomposition procedure up to two-loop order. The second root of the real-world interpretation is that the replica currents $\vec{\lambda}$ are conserved in each vertex just as currents are conserved in nodes of real networks. Hence we may write for each edge i of a diagram $\vec{\lambda}_i = \vec{\lambda}_i(\vec{\lambda},\{\vec{\kappa}\})$, where $\vec{\lambda}$ is an external current and $\{\vec{\kappa}\}$ denotes a complete set of independent loop currents. The $\vec{\lambda}$-dependent part of each conducting diagram then takes the form

$$\exp\Big[\rho w_r\sum_i t_i\Lambda_r(\vec{\lambda}_i)\Big]. \tag{3.7}$$

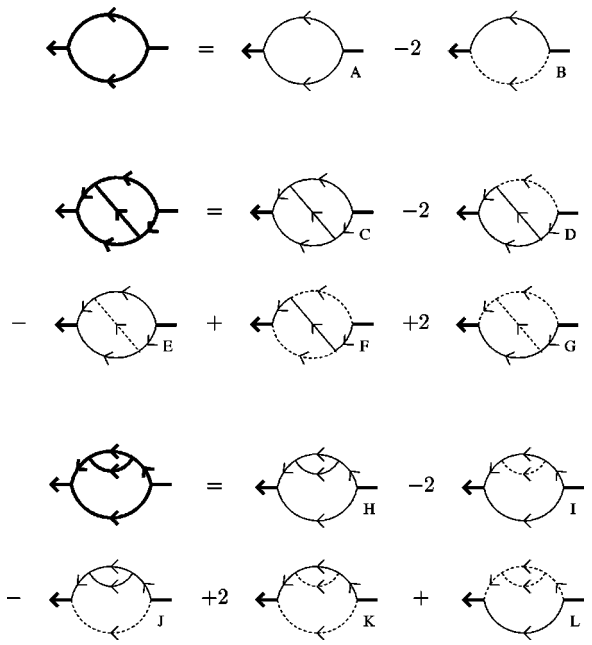

FIG. 1. Decomposition of the primary two-leg diagrams (bold) into conducting diagrams composed of conducting (light) and insulating (dashed) propagators to two-loop order. It is important to realize that the conducting diagrams inherit their combinatorial factor from their bold diagram. For example, the diagrams A and B have to be calculated with the same combinatorial factor $\frac{1}{2}$.

Now it is important to realize that $\Sigma_i t_i \Lambda_r(\vec{\lambda}_i)$ resembles the structure of a power [cf. Eq. (2.6)]. Thus, we interpret the ''time'' associated with a conducting propagator as its resistance and write

$$[\text{Eq. (3.7)}] = \exp[\rho w_r P_r(\vec{\lambda},\{\vec{\kappa}\})]. \tag{3.8}$$

The real-world interpretation provides for an alternative way of computing the conducting Feynman diagrams. To evaluate the sums over independent loop currents

$$\sum_{\{\vec{\kappa}\}} \exp[\rho w_r P_r(\vec{\lambda},\{\vec{\kappa}\})], \tag{3.9}$$

we employ the saddle point method under the conditions discussed at the end of Sec. II C. Note that the saddle point equation is nothing more than the variational principle stated in Eq. (2.7). Thus, solving the saddle point equations is equivalent to determining the total resistance $R_r(\{t_i\})$ of a diagram, and the saddle point evaluation of Eq. (3.9) yields

$$\exp[R_r(\{t_i\})\rho w_r \Lambda_r(\vec{\lambda})], \tag{3.10}$$

where we have omitted once more multiplicative factors that go to 1 for $D \to 0$. A completion of squares in the momenta renders the momentum integrations, which remain to be done to compute the diagrams, straightforward. Equally well we can use the saddle point method which is exact here since the momentum dependence is purely quadratic. After an expansion for small $w_r \Lambda_r(\vec{\lambda})$ all diagrammatic contributions are of the form

$$\begin{aligned} I(\mathbf{p}^2,t,\Lambda_r(\vec{\lambda})) &= I_P(\mathbf{p}^2,t) + I_W(\mathbf{p}^2,t)\rho w_r \Lambda_r(\vec{\lambda}) + \cdots \\ &= \int_0^\infty \prod_i dt_i [1 + R_r(\{t_i\})\rho w_r \Lambda_r(\vec{\lambda}) \\ &\quad + \cdots] D(\mathbf{p}^2,t;\{t_i\}). \end{aligned} \tag{3.11}$$

$D(\mathbf{p}^2,t;\{t_i\})$ is a typical integrand as known from the field theory of DP [20–22].

B. Renormalization and scaling

We proceed with standard techniques of renormalized field theory [26]. The ultraviolet divergences occurring in the diagrams can be absorbed by dimensional regularization. We employ the renormalization scheme

$$s \to \mathring{s} = Z^{1/2} s, \quad \tau \to \mathring{\tau} = Z^{-1} Z_\tau \tau, \tag{3.12a}$$

$$w_r \to \mathring{w}_r = Z^{-1} Z_{w_r} w_r, \quad \rho \to \mathring{\rho} = Z^{-1} Z_\rho \rho, \tag{3.12b}$$

$$\overline{g} \to \mathring{\overline{g}} = Z^{-1/2} Z_\rho^{-1} Z_u^{1/2} G_\epsilon^{-1/2} u^{1/2} \mu^{\epsilon/2}, \tag{3.12c}$$

where $\epsilon = 4 - d_\perp$ and μ is the usual inverse length scale. The factor $G_\epsilon = (4\pi)^{-d_\perp/2}\Gamma(1+\epsilon/2)$, with Γ denoting the Gamma function, is introduced for convenience. Z, Z_τ, Z_ρ, and Z_u are the usual DP Z factors known to second order in ϵ [21,22,14]. In Ref. [14] we determined $Z_w = Z_{w_1}$ to second order in ϵ. Here, we calculate Z_{w_r} for arbitrary r to order ϵ. This calculation is straightforward because we can determine the total resistance of the one-loop diagrams by using simple rules. For example, two nonlinear resistors with resistances t_1 and t_2 added in series have a total resistance R_r given by

$$R_r(t_1,t_2) = t_1 + t_2, \tag{3.13}$$

whereas two such resistors in parallel give

$$R_r(t_1,t_2)^{-s} = t_1^{-s} + t_2^{-s}. \tag{3.14}$$

By exploiting Eq. (3.14) we find

$$Z_{w_r} = 1 + \frac{u}{2\epsilon}\left[1 - \frac{1}{2^{r+1}}\right] + O(u^2). \tag{3.15}$$

Calculating Z_{w_r} for general r to higher loop orders appears to be beyond possibility. The reason is that conducting diagrams like C in Fig. 1 appear. The total resistance of these diagrams cannot be determined by using simple rules like Eqs. (3.13) and (3.14). Instead, one has to solve the set of nonlinear circuit equations, which is hardly feasible in closed form.

Now we set up in a standard fashion the renormalization group equation for our problem. The unrenormalized theory has to be independent of the length scale μ^{-1} introduced by renormalization. In particular, the unrenormalized connected N-point correlation functions must be independent of μ, i.e.,

$$\mu\frac{\partial}{\partial\mu}\mathring{G}_N(\{\mathbf{x}_\perp,\mathring{\rho}t,\mathring{w}_r\Lambda_r(\vec{\lambda})\};\mathring{\tau},\mathring{\vec{g}})=0 \tag{3.16}$$

for all N. Equation (3.16) translates via the Wilson functions

$$\beta(u)=\mu\frac{\partial u}{\partial\mu}\bigg|_0,\quad \kappa(u)=\mu\frac{\partial\ln\tau}{\partial\mu}\bigg|_0, \tag{3.17a}$$

$$\zeta_r(u)=\mu\frac{\partial\ln w_r}{\partial\mu}\bigg|_0,\quad \zeta_\rho(u)=\mu\frac{\partial\ln\rho}{\partial\mu}\bigg|_0, \tag{3.17b}$$

$$\gamma_{\ldots}(u)=\mu\frac{\partial}{\partial\mu}\ln Z_{\ldots}\bigg|_0, \tag{3.17c}$$

where the bare quantities are kept fixed while taking the derivatives, into the Gell-Mann-Low renormalization group equation

$$\left[\mu\frac{\partial}{\partial\mu}+\beta\frac{\partial}{\partial u}+\tau\kappa\frac{\partial}{\partial\tau}+w_r\zeta_r\frac{\partial}{\partial w_r}+\rho\zeta_\rho\frac{\partial}{\partial\rho}+\frac{N}{2}\gamma\right]\times G_N(\{\mathbf{x}_\perp,\rho t,w_r\Lambda_r(\vec{\lambda})\};\tau,u,\mu)=0. \tag{3.18}$$

The particular form of the Wilson functions can be extracted from the renormalization scheme and the Z factors.

The critical behavior of the correlation functions is determined by the infrared stable fixed point solutions of Eq. (3.18). This fixed point u^* is readily extracted from the condition $\beta(u^*)=0$. Then Eq. (3.18) is solved at u^* by the method of characteristics, which gives

$$G_N(\{\mathbf{x}_\perp,\rho t,w_r\Lambda_r(\vec{\lambda})\};\tau,u,\mu)=l^{\gamma^* N/2}G_N(\{l\mathbf{x}_\perp,l^{\zeta_\rho^*}\rho t,l^{\zeta_r^*}w_r\Lambda_r(\vec{\lambda})\};l^{\kappa^*}\tau,u^*,l\mu), \tag{3.19}$$

where $\gamma^*=\gamma(u^*)$, $\kappa^*=\kappa(u^*)$, $\zeta_\rho^*=\zeta_\rho(u^*)$, and $\zeta_r^*=\zeta_r(u^*)$. To analyze the scaling behavior of the correlation functions completely, the solution (3.19) has to be supplemented by a dimensional analysis:

$$G_N(\{\mathbf{x}_\perp,\rho t,w_r\Lambda_r(\vec{\lambda})\};\tau,u,\mu)=\mu^{d_\perp N/2}G_N(\{\mu\mathbf{x}_\perp,\mu^2\rho t,\mu^{-2}w_r\Lambda_r(\vec{\lambda})\};\mu^{-2}\tau,u,1). \tag{3.20}$$

Equation (3.19) in conjunction with Eq. (3.20) now gives

$$G_N(\{\mathbf{x}_\perp,\rho t,w_r\Lambda_r(\vec{\lambda})\};\tau,u,\mu)=l^{(d_\perp+\eta)N/2}\times G_N(\{l\mathbf{x}_\perp,l^z\rho t,l^{-\phi_r/\nu}w_r\Lambda_r(\vec{\lambda})\};l^{-1/\nu}\tau,u^*,\mu). \tag{3.21}$$

$\eta=\gamma^*$, $z=2+\zeta_\rho^*$, and $\nu_\perp=1/(2-\kappa^*)$ are the well known critical exponents for DP which have been calculated previously to second order in ϵ [21,22,14]. These DP exponents, however, are not sufficient to specify the critical behavior of the RDN correlation functions completely. In Eq. (3.21) we introduced the additional nonlinear resistance exponent

$$\phi_r=\nu_\perp(2-\zeta_r^*)=1+\frac{\epsilon}{3\times 2^{r+2}}+O(\epsilon^2). \tag{3.22}$$

Note that $\phi=\phi_1$ is in conformity to order ϵ with our result for the resistance exponent for the usual ''Ohmic'' RDN, i.e., Eq. (3.22) satisfies an important consistency check.

Since we are primarily interested in the critical behavior of the average two-port resistance, we now take a closer look at the two-point correlation function $G=G_2$. Equation (3.21) implies for G at $\tau=0$ that

$$G(|\mathbf{x}_\perp-\mathbf{x}'_\perp|,t-t',w_r\Lambda_r(\vec{\lambda}))=l^{d_\perp+\eta}G(l|\mathbf{x}_\perp-\mathbf{x}'_\perp|,l^z(t-t'),l^{-\phi_r/\nu}w_r\Lambda_r(\vec{\lambda})), \tag{3.23}$$

where we dropped several arguments for notational simplicity. In the following we set $\mathbf{x}'_\perp=\mathbf{0}$ and $t'=0$, once more for the sake of simplicity. The choice $l=|\mathbf{x}_\perp|^{-1}$ and a Taylor expansion of the right hand side of Eq. (3.23) lead to

$$G(|\mathbf{x}_\perp|,t,w_r\Lambda_r(\vec{\lambda}))=|\mathbf{x}_\perp|^{1-d-\eta}f_1\left(\frac{t}{|\mathbf{x}_\perp|^z}\right)\times\left\{1+w_r\Lambda_r(\vec{\lambda})|\mathbf{x}_\perp|^{\phi_r/\nu_\perp}f_{w,1}\left(\frac{t}{|\mathbf{x}_\perp|^z}\right)+\cdots\right\}, \tag{3.24}$$

where $\nu_\parallel=\nu_\perp z$ and where the f's are scaling functions. Equally well we can choose $l=t$ which then leads to

$$G(|\mathbf{x}_\perp|,t,w_r\Lambda_r(\vec{\lambda}))=t^{(1-d-\eta)/z}f_2\left(\frac{|\mathbf{x}_\perp|^z}{t}\right)\times\left\{1+w_r\Lambda_r(\vec{\lambda})t^{\phi_r/\nu_\parallel}f_{w,2}\left(\frac{|\mathbf{x}_\perp|}{t}\right)+\cdots\right\} \tag{3.25}$$

with other scaling functions f_2 and $f_{w,2}$.

Now we can extract the critical behavior of M_{R_r}. For measurements in the distinguished direction we straightforwardly exploit Eq. (3.25) via Eq. (2.25) and find that

$$M_{R_r}\sim t^{\phi_r/\nu_\parallel}. \tag{3.26}$$

For all other directions we determine M_{R_r} from Eq. (3.24). With the help of Eq. (2.25) we find that

$$M_{R_r}\sim|\mathbf{x}_\perp|^{\phi_r/\nu_\perp}f_{w,1}\left(\frac{t}{|\mathbf{x}_\perp|^z}\right). \tag{3.27}$$

Here it is convenient to choose a common length scale L and to express both $|\mathbf{x}_\perp|$ and t in terms of it: $|\mathbf{x}_\perp| \sim L$ and $t \sim L^z$. This choice guarantees that the scaling function $f_{w,1}$ is constant and Eq. (3.27) simplifies to

$$M_{R_r} \sim L^{\phi_r/\nu_\perp}. \tag{3.28}$$

IV. FRACTAL DIMENSIONS OF DP CLUSTERS

In this section we calculate ϕ_r for $r \to 0^+$, $r \to \infty$, and $r \to -1^+$ to two-loop order. This provides us with the fractal dimension of the backbone, the red bonds, and the chemical length, respectively.

A. Red bonds

For self-affine objects the notion of fractal dimension is less straightforward than for self-similar objects. To determine, for example, the fractal dimension of the red bonds in DP one considers a $(d-1)$-dimensional hyperplane with orientation perpendicular to $x_\parallel$. The cut through the red bonds is a self-similar object with the fractal dimension

$$d_{\mathrm{red}}^{\mathrm{cut}} = d_{\mathrm{red}} - 1, \tag{4.1}$$

where d_{red} is the local fractal dimension [32] of the red bonds. By virtue of Eqs. (2.12) and (3.27) the mass of the red bonds scales as

$$M_{\mathrm{red}} = |\mathbf{x}_\perp|^{\phi_\infty/\nu_\perp} f_{w,1}\left(\frac{x_\parallel}{|\mathbf{x}_\perp|^z}\right). \tag{4.2}$$

Accordingly the mass of the cut scales as

$$M_{\mathrm{red}}^{\mathrm{cut}} = |\mathbf{x}_\perp|^{\phi_{-1}/\nu_\perp} x_\parallel^{-1} f_{w,1}\left(\frac{x_\parallel}{|\mathbf{x}_\perp|^z}\right). \tag{4.3}$$

By choosing once more $|\mathbf{x}_\perp| \sim L$ and $x_\parallel \sim L^z$ we find that

$$M_{\mathrm{red}}^{\mathrm{cut}} \sim L^{\phi_\infty/\nu_\perp - z}. \tag{4.4}$$

This leads via Eq. (4.1) to

$$d_{\mathrm{red}} = 1 + \phi_\infty/\nu_\perp - z. \tag{4.5}$$

It remains to compute ϕ_∞. To do so we take direct advantage of our view of the Feynman diagrams as being resistor networks themselves. As argued in Sec. II B, blobs do not contribute to the total resistance for $r \to \infty$. In analogy

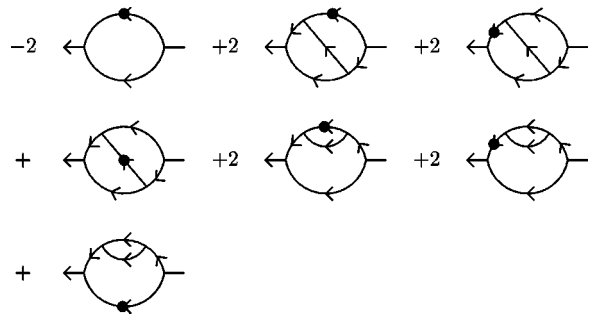

FIG. 2. Diagrammatic expansion in the limit $r \to \infty$. The listed diagrams including their prefactors can be obtained from the conducting diagrams shown in Fig. 1 in two different ways: first by inserting $\frac{1}{2}s^2$ into all singly connected conducting propagators and second by inserting $\frac{1}{2}s^2$ into every conducting and insulating propagator. As a consequence, the renormalization factors Z_{w_∞} and Z_τ are identical. The lines stand for conducting propagators evaluated at zero currents, the solid dots for $\frac{1}{2}s^2$ insertions.

only singly connected conducting propagators contribute to the total resistance of a diagram, i.e.,

$$R_\infty(\{t_i\}) = \sum_i^{\mathrm{singly}} t_i, \tag{4.6}$$

with the sum being taken exclusively over singly connected conducting propagators. The contribution of a diagram to the renormalization factor Z_{w_∞} takes the form

$$I_W(\mathbf{p}^2,t) = \int_0^\infty \prod_j dt_j D(\mathbf{p}^2,t;\{t_j\}) \sum_i^{\mathrm{singly}} t_i. \tag{4.7}$$

Note that the factor t_i in Eq. (4.7) corresponds to the insertion (cf. Ref. [26]) of $\frac{1}{2}s^2$ into the ith edge of the diagram. Thus, we can generate $I_W(\mathbf{p}^2,t)$ for a given conducting diagram by inserting $\frac{1}{2}s^2$ into its singly connected conducting propagators. This procedure is carried out up to two-loop order, i.e., every conducting propagator in Fig. 1 that does not belong to a closed loop gets an insertion. The resulting diagrams are displayed in Fig. 2.

At this point it is instructive to consider the contributions of the diagrams listed in Fig. 1 to Z_τ. These can be generated by inserting $\frac{1}{2}s^2$ in conducting as well as in insulating propagators. Again, one obtains the diagrams depicted in Fig. 2 with the same prefactors. Consequently, Z_{w_∞} and Z_τ are identical at least up to two-loop order. The same goes for the corresponding Wilson functions ζ_∞ and κ. From the definition of ϕ_r it follows that

$$\phi_\infty = \frac{2-\zeta_\infty^*}{2-\kappa^*} = 1 + O(\epsilon^3). \tag{4.8}$$

Upon inserting Eq. (4.8) into Eq. (4.5) we obtain the principal result of Sec. IV A,

$$d_{\mathrm{red}} = 1 + 1/\nu_\perp - z, \tag{4.9}$$

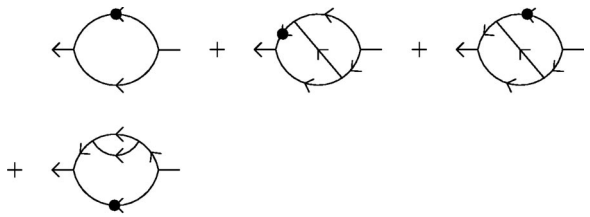

FIG. 3. Diagrammatic expansion in the limit $r \to 0^+$. The meaning of the symbols is the same as in Fig. 2.

holding at least to second order in ϵ. By substituting the results of Refs. [21,22] in Eq. (4.9) we obtain the following ϵ expansion for d_{red}:

$$d_{\mathrm{red}} = 1 - \frac{\epsilon}{6}\left\{1 + \left[\frac{73}{288} - \frac{55}{144}\ln\left(\frac{4}{3}\right)\right]\epsilon\right\} + O(\epsilon^3). \tag{4.10}$$

Note that the scaling relation (4.9) holds rigorously and its validity is not restricted to second order in the ϵ expansion. Coniglio [33] proved for IP that the mass of the red bonds scales as

$$M_{\mathrm{red}}(\mathbf{0},\mathbf{x}) \sim |\mathbf{x}|^{1/\nu}. \tag{4.11}$$

For IP this is equivalent to saying that the fractal dimension of the red bonds is $d_{\mathrm{red}} = 1/\nu$. Since Coniglio's arguments do not rely on the isotropy of the system, they can be adapted to apply to DP. For the DP problem Eq. (4.11) has to be modified to

$$M_{\mathrm{red}}(\mathbf{0},\mathbf{x}) = |\mathbf{x}_\perp|^{1/\nu_\perp} f_{w,1}\left(\frac{x_\parallel}{|\mathbf{x}_\perp|^z}\right). \tag{4.12}$$

This in turn leads again to Eq. (4.9).

B. Chemical length

Next we address the fractal dimension of the chemical length. Equation (2.15) in conjunction with Eq. (3.27) provides us with

$$M_{\mathrm{min}} = |\mathbf{x}_\perp|^{\phi_0/\nu_\perp} f_{w,1}\left(\frac{x_\parallel}{|\mathbf{x}_\perp|^z}\right). \tag{4.13}$$

By applying the same reasoning as in Sec. IV C we learn that the local fractal dimension of the chemical length is given by

$$d_{\mathrm{min}} = 1 + \phi_0/\nu_\perp - z. \tag{4.14}$$

In order to calculate ϕ_0 we determine the shortest self-avoiding path of conducting propagators connecting the external legs of a diagram. Due to the dynamic structure all of these paths for a given diagram have the same total resistance which is nothing more than the total ''time'' between the external legs. Hence we can choose any self-avoiding path connecting the external legs. We work with the diagrammatic expansion depicted in Fig. 3.

Minimal subtraction provides us with the renormalization factor

$$Z_0 = 1 + \frac{u}{4\epsilon} + \frac{u^2}{32\epsilon}\left[\frac{7}{\epsilon} - 3 + \frac{9}{2}\ln\left(\frac{4}{3}\right)\right] + O(u^3). \tag{4.15}$$

Note that Z_0 as stated in Eq. (4.15) is identical to the field renormalization Z given to two-loop order in Refs. [21,22,14]. By virtue of the renormalization scheme (3.12) we deduce that

$$\mathring{\rho}\mathring{w}_0 = \rho w_0, \tag{4.16}$$

at least to second order in u. Equation (4.16) leads via

$$\mu \frac{\partial \ln(\rho w_0)}{\partial \mu}\bigg|_0 = 0 \tag{4.17}$$

to

$$\zeta_\rho + \zeta_0 = 0. \tag{4.18}$$

From the definitions of ϕ_r and z it follows immediately that

$$\phi_0 = \nu_\perp z + O(\epsilon^3). \tag{4.19}$$

In conjunction with Eq. (2.15) this leads finally to

$$d_{\mathrm{min}} = 1 + O(\epsilon^3). \tag{4.20}$$

This result is intuitively plausible because the chemical distance in DP is basically equivalent to the ''time'' t.

C. Backbone

We conclude Sec. IV by studying the backbone dimension. By virtue of Eqs. (2.9) and (3.27) the mass of the backbone scales as

$$M_B = |\mathbf{x}_\perp|^{\phi_{-1}/\nu_\perp} f_{w,1}\left(\frac{x_\parallel}{|\mathbf{x}_\perp|^z}\right). \tag{4.21}$$

Accordingly the local fractal dimension of the backbone is given by

$$D_B = 1 + \phi_{-1}/\nu_\perp - z. \tag{4.22}$$

It remains to compute ϕ_{-1}. Once more we exploit our real-world interpretation. As argued in Sec. II B, the resistance of the backbone between two sites x and x' is given by

$$R_{-1,+}(x,x') = \sum_{\underline{b}} \rho_{\underline{b}}(I_{\underline{b}}), \tag{4.23}$$

with the sum running over all current carrying bonds of the underlying cluster. In analogy, the resistance of a conducting Feynman diagram is given by

$$R_{-1}(\{t_i\}) = \sum_i^{\mathrm{cond}} t_i, \tag{4.24}$$

where the sum extends over all conducting propagators of the diagram. This tells us that the contribution of a diagram to $Z_{w_{-1}}$ takes the form

$$I_W(\mathbf{p}^2,t)=\int_0^\infty \prod_j dt_j D(\mathbf{p}^2,t,\{t_j\}) \sum_i^{\text{cond}} t_i . \tag{4.25}$$

Hence we can generate $I_W(\mathbf{p}^2,t)$ of any conducting diagram by inserting $\frac{1}{2}s^2$ into its conducting propagators. All conducting propagators in Fig. 1 get such an insertion. Then it is a matter of simple counting to see that the individual contributions cancel each other. Thus, we find

$$Z_{w_{-1}}=1+O(\epsilon^3). \tag{4.26}$$

As a consequence we obtain

$$\lim_{r\to -1^+} \phi_r/\nu_\perp = z-\eta, \tag{4.27}$$

at least to second order in ϵ. Equation (4.27) leads by virtue of Eq. (4.22) to

$$D_B=1-\eta=d-\frac{2\beta}{\nu_\perp}, \tag{4.28}$$

where $\beta=\nu_\perp(d-1+\eta)/2$ is the DP order parameter exponent known to second order in ϵ [21,22]. From the scaling relation Eq. (4.28), which is the main result of this section, the ϵ expansion of D_B is readily obtained by inserting the ϵ expansion for η [21,22]:

$$D_B=1+\frac{\epsilon}{6}\left\{1+\left[\frac{25}{288}+\frac{161}{144}\ln\left(\frac{4}{3}\right)\right]\epsilon\right\}+O(\epsilon^3). \tag{4.29}$$

Equation (4.28) is in agreement with scaling arguments [34] yielding that the fractal dimension of the transverse cut through a DP cluster with local dimension d_f is $d_f-1=d-1-\beta/\nu_\perp$. The analogous cut through the backbone can be viewed as the intersection of the cut through the cluster and the cluster's backward oriented pendant [10,35]. Hence, the codimension of the backbone cut is twice the codimension $\beta/\nu_\perp$ of the cluster cut, which leads again to Eq. (4.28).

It is interesting to compare the ϵ expansion result to numerical estimates. We are not aware, however, of any simulations in which D_B itself was determined. Huber *et al.* [36] presented numerical results for the scaling exponent of the backbone mass when measured in the longitudinal direction. In the following we call this exponent $\tilde{D}_B$. Formally one can define $\tilde{D}_B$ via $M_B\sim t^{\tilde{D}_B}$. From Eqs. (2.9), (3.26), and (4.27) it follows that

$$\tilde{D}_B=1+\frac{2\beta}{\nu_\parallel}+\frac{d-1}{z}, \tag{4.30}$$

at least to second order in ϵ. Crudely evaluating the corresponding ϵ expansion of $\tilde{D}_B$ for small spatial dimensions leads to poor quantitative predictions. Therefore it is appropriate to improve the ϵ-expansion by incorporating rigorously known features. We carry out a rational approximation which takes into account that obviously $\tilde{D}_B(d=1)=1$. In practice this is done by adding an appropriate third order term. By this procedure we obtain the interpolation formula

$$\tilde{D}_B\approx 1+\left(1-\frac{\epsilon}{4}\right)(0.0833\epsilon+0.0583\epsilon^2). \tag{4.31}$$

Evaluation in two dimensions leads to $\tilde{D}_B(d=2)=1.2\pm 0.15$, where the error is based on a subjective estimate. This result is, within the errors, in agreement with the numerical result [36] $\tilde{D}_B(d=2)=1.30\pm 0.03$. Our result, though, appears to be somewhat small.

V. CONCLUSIONS

In this paper we studied a nonlinear version of resistor diode percolation where Ohm's law is generalized to $V\sim I^r$. We investigated the critical behavior of the average two-port resistance M_{R_r} at the transition from the nonpercolating to the directed percolating phase. By employing our real-world interpretation of Feynman diagrams we calculated the resistance exponent ϕ_r for arbitrary r to one-loop order. To our knowledge this is the first time that ϕ_r has been determined for the RDN while ϕ_r has been known for the RRN, also to one-loop order, since the 1980s [18]. Extending either of these results to higher loop orders seems to be beyond possibility because not all conducting diagrams appearing at higher loop orders can be assembled by simply adding resistors in parallel and in series. For these diagrams one has to solve the set of nonlinear Kirchhoff's equations to obtain their total resistance. In closed form, however, this is hardly feasible.

The relation of M_{R_r} to the mass of the red bonds, the chemical length, and the backbone, respectively, provided us with alternative means to extract the fractal dimensions of these substructures of DP clusters. By computing ϕ_r for $r\to\infty$, $r\to 0^+$, and $r\to -1^+$ we determined d_{red}, $d_{\min}$, and D_B to two-loop order.

The fractality in DP and IP is qualitatively different. DP clusters are self-affine rather than self-similar objects. Hence, the notion of fractal dimension is more subtle for DP than for IP. Moreover, DP has a Markovian character which is evident in the dynamic interpretation. This Markovian character provides for scaling relations that do not have an analog in IP. The DP backbone dimension, for example, can be expressed entirely in terms of the usual (purely geometric) critical exponents of the DP universality class, $D_B=d-2\beta/\nu_\perp$. Within the renormalization group framework such a scaling relation is typically associated with a Ward identity. The fact that w_{-1} renormalizes trivially to two-loop order is reminiscent of this Ward identity. It is an interesting issue for future work to identify the Ward identity and its underlying symmetry. Another consequence of the Markovian character of DP is that the fractal dimension of the chemical length is identical to 1. This is intuitively plausible since the shortest longitudinal path through a DP cluster corresponds to the time in the dynamical interpretation.

The fractal dimension of the red bonds in DP obeys the scaling relation $d_{\mathrm{red}}=1+1/\nu_{\perp}-z$, similar to the $d_{\mathrm{red}}=1/\nu$ for IP. The Ward identities corresponding to either of these scaling relations are not known to date. Again, this leaves interesting and challenging opportunities for future studies.

ACKNOWLEDGMENT

We acknowledge support by the Sonderforschungsbereich 237 ''Unordnung und große Fluktuationen'' of the Deutsche Forschungsgemeinschaft.

[1] For a review on percolation see, e.g., A. Bunde and S. Havlin, *Fractals and Disordered Systems* (Springer, Berlin, 1991); D. Stauffer and A. Aharony, *Introduction to Percolation Theory* (Taylor and Francis, London, 1992); B. D. Hughes, *Random Walks and Random Environments* (Clarendon, Oxford, 1995).
[2] For a review on DP see, e.g., H. Hinrichsen, Adv. Phys. **49**, 815 (2000).
[3] N. Van Lien and B. I. Shklovskii, Solid State Commun. **38**, 99 (1981).
[4] J. Kertész and T. Vicsek, J. Phys. C **13**, L343 (1980).
[5] See, e.g., A.-L. Barabasi *et al.*, in *Surface Disordering: Growth, Roughening, and Phase Transitions*, edited by R. Jullien *et al.* (Nova Science, New York, 1992); S. Havlin *et al.*, in *Growth Patterns*, edited by J. M. Garcia-Ruiz *et al.* (Plenum, New York, 1993).
[6] See, e.g., J. D. Murray, *Mathematical Biology* (Springer, Berlin, 1988).
[7] P. Grassberger, J. Phys. A **18**, L215 (1985).
[8] K. Sneppen and M. H. Jensen, Phys. Rev. Lett. **70**, 3833 (1993); **71**, 101 (1993); Phys. Rev. E **49**, 919 (1994); P. Bak and K. Sneppen, Phys. Rev. Lett. **71**, 4083 (1993); M. Paczuski, S. Maslov, and P. Bak, Europhys. Lett. **27**, 97 (1994).
[9] S. Redner, J. Phys. A **14**, L349 (1981); Phys. Rev. B **25**, 3242 (1982).
[10] S. Redner, in *Percolation Structures and Processes*, edited by G. Deutscher *et al.* (Adam Hilger, Bristol, 1983).
[11] RDNs were already contained implicitly in the pioneering work of S. R. Broadbent and J. M. Hammersley on percolation [Proc. Cambridge Philos. Soc. **53**, 629 (1957)].
[12] H. K. Janssen and O. Stenull, Phys. Rev. E **62**, 3173 (2000).
[13] H. K. Janssen and O. Stenull, Phys. Rev. E **63**, 025103(R) (2001).
[14] O. Stenull and H. K. Janssen, J. Stat. Phys. (to be published).
[15] See also S. W. Kenkel and J. P. Straley, Phys. Rev. Lett. **49**, 767 (1982).
[16] R. Blumenfeld and A. Aharony, J. Phys. A **18**, L443 (1985).
[17] M. J. Stephen, Phys. Rev. B **17**, 4444 (1978).
[18] A. B. Harris, Phys. Rev. B **35**, 5056 (1987).
[19] See, e.g., A. B. Harris and T. C. Lubensky, Phys. Rev. B **35**, 6964 (1987).
[20] J. L. Cardy and R. L. Sugar, J. Phys. A **13**, L423 (1980).
[21] H. K. Janssen, Z. Phys. B: Condens. Matter **42**, 151 (1981).
[22] H. K. Janssen, e-print cond-mat/0006129.
[23] H. K. Janssen, Z. Phys. B **23**, 377 (1976); R. Bausch, H. K. Janssen, and H. Wagner, *ibid.* **24**, 113 (1976); H. K. Janssen, in *Dynamical Critical Phenomena and Related Topics*, Vol. 104 of Lecture Notes in Physics, edited by C. P. Enz, (Springer, Heidelberg, 1979).
[24] C. De Dominicis, J. Phys. (Paris), Colloq. **37**, C-247 (1976); C. De Dominicis and L. Peliti, Phys. Rev. B **18**, 353 (1978).
[25] H. K. Janssen, in *From Phase Transitions to Chaos*, edited by G. Györgyi, I. Kondor, L. Sasvári, and T. Tél (World Scientific, Singapore, 1992).
[26] See, e.g., D. J. Amit, *Field Theory, the Renormalization Group, and Critical Phenomena* (World Scientific, Singapore, 1984); J. Zinn-Justin, *Quantum Field Theory and Critical Phenomena* (Clarendon, Oxford, 1989).
[27] O. Stenull, H. K. Janssen, and K. Oerding, Phys. Rev. E **59**, 4919 (1999).
[28] H. K. Janssen, O. Stenull, and K. Oerding, Phys. Rev. E **59**, R6239 (1999).
[29] H. K. Janssen and O. Stenull, Phys. Rev. E **61**, 4821 (2000).
[30] O. Stenull, *Renormalized Field Theory of Random Resistor Networks* (Shaker, Aachen, 2000).
[31] O. Stenull and H. K. Janssen, Europhys. Lett. **51**, 539 (2000).
[32] See, e.g., J. Kertész, and T. Vicsek, in *Fractals in Science*, edited by A. Bunde and S. Havlin (Springer, Berlin, 1994).
[33] A. Coniglio, Phys. Rev. Lett. **46**, 250 (1981); J. Phys. A **15**, 3829 (1982).
[34] See, e.g., B. Hede, J. Kertész, and T. Vicsek, J. Stat. Phys. **64**, 829 (1991).
[35] B. M. Arora, M. Barma, D. Dhar, and M. K. Phani, J. Phys. C **16**, 2913 (1983).
[36] G. Huber, M. H. Jensen, and K. Sneppen, Phys. Rev. E **52**, R2133 (1995).